








Exploring the Potential of Deep-Learning and Machine-Learning in Dual-Band Antenna Design

RIDA GADHAFI ¹ (Senior Member, IEEE), ABIGAIL COPIACO ¹ (Member, IEEE),
YASSINE HIMEUR ¹ (Senior Member, IEEE), KIYAN AFSARI ² (Member, IEEE),
HUSAMELDIN MUKHTAR ¹ (Senior Member, IEEE), KHALIDA GHANEM ^{3,4},
AND WATHIQ MANSOOR ¹ (Senior Member, IEEE)

¹College of Engineering and IT, University of Dubai, Dubai 14143, UAE

²School of Engineering, University of Wollongong in Dubai, Dubai 20183, UAE

³University of Quebec en Abitibi Témiscamingue (UQAT), Rouyn-Noranda, QC J9X5E4, Canada

⁴Telecom Division, Center for Development of Advanced Technologies (CDTA), Baba Hassen 16081, Algeria

CORRESPONDING AUTHOR: RIDA GADHAFI (e-mail: rgadhafi@ud.ac.ae).

ABSTRACT This article presents an in-depth exploration of machine learning (ML) and deep learning (DL) for the optimization and design of dual-band antennas in Internet of Things (IoT) applications. Dual-band antennas, which are essential for the functionality of current and forthcoming flexible wireless communication systems, face increasing complexity and design challenges as demands and requirements for IoT-connected devices become more challenging. The study demonstrates how artificial intelligence (AI) can streamline the antenna design process, enabling customization for specific frequency ranges or performance characteristics without exhaustive manual tuning. By utilizing ML and DL tools, this research not only enhances the efficiency of the design process but also achieves optimal antenna performance with significant time savings. The integration of AI in antenna design marks a notable advancement over traditional methods, offering a systematic approach to achieving dual-band functionality tailored to modern communication needs. We approached the antenna design as a regression problem, using the reflection coefficient, operating frequency, bandwidth, and voltage standing wave ratio as input parameters. The ML and DL models then are used to predict the corresponding design parameters for the antenna by using 1,000 samples, from which 700 are allocated for training and 300 for testing. This effectiveness of this approach is demonstrated through the successful application of various ML techniques, including Fine Gaussian Support Vector Machines (SVM), as well as Regressor and Residual Neural Networks (ResNet) with different activation functions, to optimize the design of a dual-band T-shaped monopole antenna, thereby substantiating AI's transformative potential in antenna design.

INDEX TERMS Machine learning, deep learning, antenna design, dual-band antennas, AI-antenna.

I. INTRODUCTION

The Internet of Things (IoT) has become indispensable in the modern world, as many systems fully integrated into our daily lives are wirelessly connected and supported by IoT devices [1], [2]. In such systems, as in any wireless communication system, antennas play a crucial role, significantly impacting the quality and range of signal transmission and reception over distances [3]. Therefore, it is essential to use

highly optimized antennas designed to meet the sophisticated requirements of these systems to ensure better signal quality.

With the growing demand for IoT-connected devices and systems, along with the high data rates required by current applications, the need for multiple antennas has surged. However, as the number of antennas increases, the system complexity follows the same trend. This leads to a higher need for antennas capable of operating in multiple bands,

simplifying the system. The recent boom in artificial intelligence (AI) has further advanced the development of AI-enabled antennas [4], [5], [6], [7], [8]. AI is increasingly being used to tackle complex design and optimization problems, not only in the radio frequency (RF) domain but also in various other fields. However, designing an optimized antenna for specific requirements or applications remains challenging due to the extensive labor involved, including the meticulous optimization process.

Leveraging AI techniques for antenna design aims to produce optimized solutions for various frequencies or performance parameters. AI can be exploited to deliver complete design parameters or to optimize key parameters, enabling the creation of dual-band antennas. These antennas are particularly valuable due to their ability to operate in multiple bands with AI-enabled frequency scalability.

The literature highlights significant progress in leveraging machine learning (ML) and deep learning (DL) techniques for antenna design. AI has been incorporated into the antenna field at two primary levels. The first level involves AI to predict antenna characteristics, such as operating frequency, bandwidth, and gain, based on a set of design parameters. In this case, AI optimizes and accelerates the design process. For example, [1] presents an efficient, flexible, and reliable framework to identify optimal design parameters using various ML techniques, such as Least Absolute Shrinkage and Selection Operator (LASSO), Artificial Neural Networks (ANNs), and K-Nearest Neighbor (KNN), for the design and optimization of a dual-band T-shaped monopole antenna. Similarly, in [9], the authors utilized a modified K-nearest algorithm to optimize antenna parameters, achieving reasonable results through training and testing.

The second level of AI involvement pertains to the prediction of design parameters necessary to achieve desired antenna characteristics. This approach is particularly effective for designing various antenna types based on specific requirements. While this method is less commonly applied to dual-band or multi-band antennas, where multiple design parameters are required to ensure desired multiband performance, it holds significant potential. For instance, [5] explores the use of ML to simplify the design of dielectric-filled Slotted Waveguide Antennas (SWA) with specific side lobe level ratios. The authors proposed treating the design process as a regression problem, where an ML model predicts SWA design parameters based on input specifications such as side lobe ratio, reflection coefficient, operating frequency, and dielectric material's relative permittivity, achieving high design accuracy. Similarly, [8] proposes an ML-based framework to identify optimal design parameters for a wideband monopole antenna with filtering notches, capable of resonating at multiple bands. By incorporating design parameters as input variables, the authors employed an ML algorithm to predict the antenna's reflection coefficient and efficiency curve without relying on any electromagnetic tools.

In addition to the models mentioned above, the literature contains numerous AI-enabled antenna designs, both as

stand-alone systems [10], [11], [12] and in array configurations [7], [13], [14]. One such study demonstrates the design of a single-band printed dipole antenna with an elliptical shape using a neural network approach [15]. The neural network, consisting of an input layer, one hidden layer, and an output layer, was trained on a dataset of 24 samples collected from an electromagnetic tool. The dataset was divided into 90% for training, 5% for testing, and 5% for validation, achieving minimal error in the predictions.

Thus, it is evident that AI is sometimes used for optimization purposes and other times for design purposes. These models are often associated with antennas featuring complex design equations or for optimizing specific figures of merit. Developing ML or DL approaches that can handle arbitrary designs unsupported by standard equations is crucial. Additionally, the datasets used in reported models are typically limited, as are the output parameters. It is important to maximize the number of output parameters based on given inputs. While handling multiple output models can be challenging, a cascaded approach can be effective if the outputs are interrelated [16].

In this article, we present a DL approach for designing a dual-band antenna. The antenna characteristics provided at the DL input include the operating frequency, bandwidth, minimum value of the reflection coefficient (S_{11}), and the Voltage Standing Wave Ratio (VSWR) at the operating frequency. At the DL output, four common design parameters for both bands were generated, along with six additional design parameters exclusively for producing the second band. The dual-band L-strip antenna comprises a traditional quarter-wave monopole antenna and an L-shaped strip. The first band of operation is generated by the quarter-wave monopole, while the L-strip, coupled with the monopole, produces the second band. A dataset of 1,000 samples was generated, with 70% used for training and the remainder for testing.

II. LITERATURE REVIEW: ML FOR ENHANCED ANTENNA DESIGN AND OPTIMIZATION

ML, such as Support Vector Machines (SVM) offers significant potential for enhancing antenna design and optimization by automating and improving the efficiency of these processes. Traditional antenna design relies heavily on expert knowledge and extensive simulations, which are often time-consuming and computationally expensive. In contrast, ML algorithms streamline this process by learning from vast datasets of antenna designs and performance metrics, enabling the prediction of optimal design parameters. Techniques such as neural networks, genetic algorithms, and reinforcement learning can be employed to explore complex design spaces, identify innovative configurations, and optimize performance criteria such as gain, bandwidth, and radiation patterns. By integrating ML, antenna design can achieve higher precision, faster development cycles, and novel solutions that may be difficult to discover through conventional methods.

For instance, Liu et al. (2013) introduced a surrogate model based on assisted differential evolution for antenna synthesis,

effectively reducing the need for computationally expensive electromagnetic (EM) simulations [17]. Similarly, Chen et al. (2022) presented a multibranch ML-assisted optimization method to tackle computational complexity in antenna design, striking a balance between exploration and exploitation [18]. Sharma et al. (2020) explored various ML techniques for optimizing antenna design and compared their accuracy with traditional simulation tools [1]. Zhong et al. (2022) proposed an ML-based generative method for antenna design optimization, utilizing a flexible geometric scheme to achieve significant design efficiency [19]. Additionally, Patel et al. (2022) focused on the use of ML for smart antenna design, specifically for modern communication technologies in metamaterial-based antennas [20]. Wu et al. (2024) combined different ML methods to improve the efficiency of antenna geometry design, showcasing the use of surrogate models alongside full-wave simulations [14]. Sharma et al. (2022) further explored ML optimization methods to model antenna gain performance, demonstrating improved computational efficiency and accuracy in antenna design [21].

Several recent works have applied advanced ML strategies to antenna simulations, significantly enhancing both the design process and the performance of the resulting antennas. Montaser et al. (2021) implemented a deep neural network to optimize dual-band antenna designs for 5G applications, utilizing advanced optimization algorithms to achieve high performance [12]. Testolina et al. (2019) developed an ML-based approach to emulate complex simulators, enabling rapid optimization of millimeter wave (mmWave) cellular systems [22]. Wu et al. (2021) introduced a multilayer ML-assisted optimization method for robust antenna and array design, which significantly accelerates the design process while maintaining accuracy [23]. Aoad et al. (2021) designed a multiband rectangular microstrip antenna using ML to improve both design accuracy and computational efficiency [24]. These advanced strategies demonstrate the growing capability of ML in enhancing antenna simulations, especially for complex systems and next-generation wireless technologies.

Beyond design optimization, ML has been applied to solve broader theoretical and practical challenges in antenna technology. Lin et al. (2019) proposed a DL-based beamforming design for large-scale antenna arrays, addressing Multiple-Input Multiple-Output (MIMO) design challenges in millimeter wave communication systems [25]. Similarly, Wu et al. (2020) proposed a multistage collaborative ML method for efficient multi-objective antenna modeling and optimization, utilizing various Gaussian process regression models to address the complexity of modern antenna systems [26]. These innovative applications highlight the versatility of ML in addressing both practical challenges in design and broader theoretical issues in antenna technology.

Table 1 provides a comparative analysis of different ML solutions reported in the literature for antenna design. The table categorizes these studies based on the ML models used, the datasets involved, their key contributions, limitations, and the best performance achieved. By identifying the limitations

of each study, we can outline potential directions for future research.

For example, the reliance on high-quality surrogate models in [17] can be problematic if the initial model quality is poor, potentially leading to sub-optimal optimization outcomes. Future research could focus on developing more robust surrogate models that can deliver reliable predictions even with lesser data quality or explore hybrid models that combine multiple types of predictive models to enhance reliability and accuracy across different scenarios. Similarly, [18] addresses computational complexities with a multi-branch strategy, which itself introduces complexity in implementation. Future efforts could focus on simplifying the integration of such strategies, perhaps through automated tools that assist in setting up and managing multi-branch optimization processes, making them more accessible and less prone to errors. Moving forward, our proposed approach, highlighted in the last row of the table, provides a benchmark for comparison against other existing methods, showcasing the potential for further improvements in antenna design through ML-based optimization techniques.

Another significant limitation observed in studies like [19] and [14] is their heavy dependence on large, high-quality training datasets. This reliance can be mitigated by employing unsupervised or semi-supervised learning methods, which are capable of operating effectively with unlabelled data, reducing the need for extensive pre-labeled datasets. Additionally, the study by [12] points out the high computational costs associated with training deep neural networks. This issue could be addressed by adopting more efficient network architectures or leveraging transfer learning, where a pre-trained model is fine-tuned rather than built from scratch. These alternatives could significantly reduce computational demands while maintaining or even improving the performance of ML models in antenna design.

III. METHODOLOGY

A. TRADITIONAL DESIGN APPROACHES FOR DUAL-BAND ANTENNA

Numerous dual-band antenna designs have been proposed in the literature to cater to a wide range of applications [28], [29], [30], [31]. These designs may or may not be supported by analytical design equations. Most dual-band antennas typically incorporate two or more resonating elements that enable their dual-band operation. The antenna structures are often created using electromagnetic simulation tools such as Computer Simulation Technology (CST), High-Frequency Structure Simulator (HFSS), or Advanced Design Systems (ADS). After the initial design phase, each antenna parameter undergoes a meticulous optimization process to achieve the desired performance. This step, however, can be time-consuming and requires significant computational power and manual effort.

In this work, the authors focus on an L-strip dual-band antenna, which is suitable for Wireless Local Area Network (WLAN), Worldwide Interoperability for Microwave Access

TABLE 1. Comparison of ML Applications in Antenna Design

Ref.	Model Used	Data Used	Main Contribution	Best Performance	Limitation
[17]	Surrogate Model Assisted Differential Evolution	EM simulations	Speed enhancement in antenna design optimization	3-7x faster than traditional methods	High dependency on quality of surrogate models
[18]	Multi-branch ML Assisted Optimization	Full-wave EM simulations	Reduction in computational complexity for antenna design	Balance between exploitation and exploration	Complexity in implementing multi-branch strategy
[1]	LASSO, ANNs, k-NN	Dual-band antenna data	Efficient identification of optimal design parameters	Verified accuracy with HFSS	Limited to specific antenna types
[19]	Generative ML method (GANs)	Simplified antenna geometries	Facilitation of multi-dimensional optimization	Enhanced efficiency in solution searching	Requires extensive training data
[20]	Extra Tree Regression	Metamaterial antennas	Smart antenna design for mobile applications	Reduction in simulation time by 80%	Focused only on metamaterial-based designs
[12]	Deep Neural Networks	Simulated BSPA data	Soft computation for dual-band antennas	Beam-steering optimization	High computational cost for DNN training
[25]	DL Based Beamforming Network	Large-scale antenna arrays	Robust BF design for mmWave communication	Significant spectral efficiency improvement	Limited to mmWave applications with specific challenges
[26]	Collaborative ML Methods	EM models of varying fidelity	Multiobjective antenna modeling	Significant reduction in optimization time	Complex integration of multiple ML methods
[22]	ML Techniques	Simulated network data	Optimization of complex systems using ML	Rapid optimization capabilities	Dependence on initial simulator accuracy
[27]	SVM, Stacking Ensemble	Various antenna types	Intelligent antenna type and parameter selection	Over 99% classification accuracy	Generalization to unseen antenna types
[23]	Multilayer ML-Assisted Optimization	Antenna and array designs	Robust design across multiple objectives	Effective robust design process	High computational resource requirement
[14]	CNN, GPR	Antenna geometry data	ML-assisted optimization for antenna geometry	Improved convergence and performance	Dependency on initial training data quality
[21]	GP Regression, ANN	Monopole antenna data	Optimization of gain performance in antennas	High accuracy in non-linear settings	Specific to configurations with dielectric materials
[24]	Various ML Models	Microstrip antenna data	Design of a multiband microstrip antenna	High prediction accuracy (MSE of 0.03)	Limited to certain high-frequency bands
[This Work]	Multi-input Multi-output Regressor Neural Network	L-strip dual band antenna	Simultaneous generation of multiple outputs from a set of inputs	Low time, computational, and resource requirements	Limited to certain antenna designs, accuracy can be further improved

(WiMAX), or sub-6 GHz Fifth Generation (5G) applications. This antenna is used as a case study to explore the potential of applying ML techniques to multi-band antenna designs [32].

1) L-STRIP DUAL-BAND ANTENNA

Fig. 1 illustrates the geometry of the proposed dual-band antenna. The antenna is constructed on a standard, low-cost FR-4 substrate, which has a dielectric constant of 4.4, a loss tangent of 0.025, and a thickness (h) of 1.6mm. The structure comprises a rectangular monopole strip fed by a 50 Ω microstrip feed line, with an L-strip integrated on the right side of the monopole strip. The overall dimensions of the antenna are $46 \times 45 \times 1.6 \text{ mm}^3$.

The monopole strip is a traditional quarter-wavelength monopole antenna designed to resonate at a center frequency of 2.45 GHz. To enable dual-band operation, the L-strip is introduced, which resonates at 5.5 GHz, thus covering the

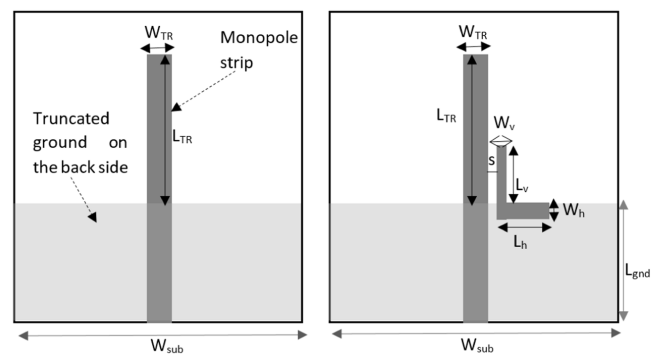


FIGURE 1. Evolution of the dual-band antenna: left) Traditional quarter-wave monopole antenna, and right) L-strip dual-band antenna.

WLAN, WiMAX, and sub-6 GHz 5G bands. The rectangular microstrip monopole, printed on the top side of the substrate, has a truncated ground plane on the bottom side, as depicted

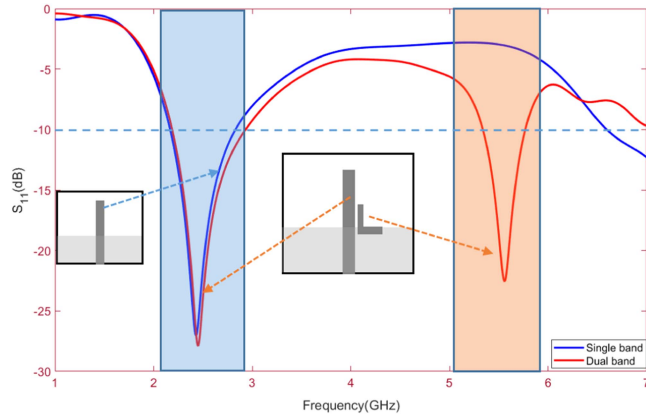


FIGURE 2. Reflection coefficients of the single and dual-band antennas.

in Fig. 1(left). The width of the radiator matches that of the feed line (W_{feed}).

The operating frequency of the monopole (f_{c1}) can be calculated using the well-known equation:

$$f_{c1} = \frac{c}{4L_{TR}\sqrt{\epsilon_{eff}}} \quad (1)$$

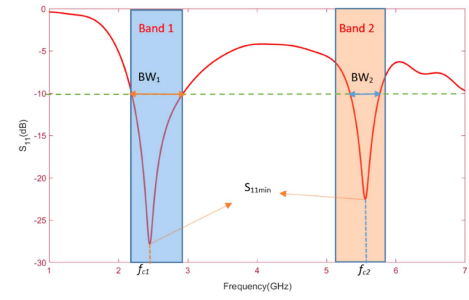
where ϵ_{eff} is the effective permittivity of the microstrip line, c is the speed of light, and L_{TR} is the length of the monopole strip.

To validate the single and dual-band operations of the antenna, simulations were performed using CST electromagnetic simulation software. Fig. 2 shows the reflection coefficients of both the single and dual-band antennas. As illustrated, the first band (f_{c1}) is generated by the monopole antenna, while coupling the monopole with the L-strip produces the second band (f_{c2}).

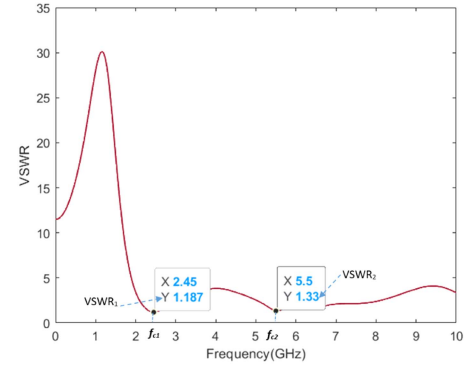
2) DATASET GENERATION

One of the primary challenges in applying ML or DL techniques to antenna design is the availability of datasets. While standard antennas may have limited datasets available, customized antennas often require the generation of in-house datasets. Given that an appropriately sized dataset is crucial for creating accurate models, the dataset used for this proposed antenna was generated using CST and comprises 1,000 data points. Of these, 700 data points were used for training and 300 for testing.

As noted in [32], the performance of the traditional monopole antenna primarily depends on four design parameters: the substrate width (W_{sub}), the length of the truncated ground plane (L_{gnd}), the monopole length (L_{TR}), and the width of the monopole (which also matches the width of the microstrip line, W_{TR}). These parameters are critical in achieving the initial band (f_{c1}). The second band (f_{c2}), on the other hand, is generated by coupling the L-strip with the monopole at a specific distance. The design parameters for this second band include the length of the ground plane (L_{gnd}), the lengths of the vertical and horizontal strips (L_v and L_h), the spacing between the L-strip and the monopole strip (s), the offset



(a) S_{11}



(b) VSWR

FIGURE 3. (a) Simulated reflection coefficient (S_{11}) and (b) VSWR of the dual-band antenna for dataset generation.

position of the L-strip from the feed point (d_{offset}), and the widths of the horizontal and vertical strips (W_v and W_h).

By varying these design parameters, the reflection coefficient (S_{11}) and Voltage Standing Wave Ratio (VSWR) of the dual-band antenna were generated using electromagnetic simulation, as shown in Fig. 3(a) and (b). The VSWR values, in particular, exhibit values less than 2 for both frequencies of operation, indicating excellent impedance matching.

Reflection coefficients were extracted from CST auto-generated. s1p files, while corresponding VSWR values were obtained by exporting. txt files. A data cleanup process was performed using MATLAB to extract the antenna's figures of merit, which include the operating frequency, bandwidth, minimum S_{11} value at the operating frequency, and the corresponding VSWR at the same frequency. The objective is to develop a model that accurately captures the relationship between these figures of merit and the design parameters.

IV. PROPOSED APPROACH

According to the data collected and the mentioned objectives, specific continuous variables are required to be estimated. Table 2 and Table 3 display the set of input features and output variables in this experiment, along with their descriptions. Note that Table 2 provides the summaries corresponding to band1, whereas Table 3 pertains to band2.

Given the data's continuous nature, a supervised learning approach must be conducted for the methodology. Supervised

TABLE 2. Summary of the Input and Output Variables Corresponding to band1

band 1 Input	Description	band 1 output	Description
S_{11min1}	min value of S_{11} at band1	L_{gnd}	ground length
f_{c1}	operating frequency of band1	W_{sub}	substrate width
BW_1	bandwidth of band1	L_{TR}	monopole length
$VSWR_1$	VSWR of band1	W_{TR}	monopole width

TABLE 3. Summary of the Input and Output Variables Corresponding to band2

Input	Description	Output	Description
S_{11min2}	Min value of S_{11} at band2	L_{gnd}	Ground length
f_{c2}	Operating frequency of band2	W_{sub}, L_{sub}	Substrate width and length
BW_2	Bandwidth of band2	L_v	Length of the vertical strip
$VSWR_2$	VSWR of band2	L_h	Length of the horizontal strip
-	-	W_v	Width of the vertical strip
-	-	W_h	Width of the horizontal strip
-	-	s	Spacing between monopole and L-strip
-	-	d_{offset}	Spacing between feed point and L-strip
-	-	L_{TR}	Length of the monopole

learning is the area of ML that relies on labeled data during the training process [33]. This approach involves providing the learning algorithm with input/s and output pairs, where the inputs are considered features, and the output is the corresponding label. By utilizing these ground truth labels, the model can learn to map inputs to their corresponding outputs, allowing for more reliable predictions when applied to unseen data.

Furthermore, since this work focuses on generating continuous variables as results, a regression technique must be retained [33]. However, it is important to note that the problem involves multi-input and multi-output data. Traditional regression techniques typically address scenarios with a single dependent variable, despite authorizing a varying number of independent variables. To accommodate this constraint, the experiment will be examined in three distinct ways:

- 1) Multiple-input, Single-output Regression Techniques: Common regression techniques were compared in our initial work [16]. These included, but were not limited to: Decision Trees, Linear Regression Techniques, and SVM. Through these experiments, it was found that Fine Gaussian SVM returned the best Root Mean Square Error (RMSE) score among the models compared. Hence, Fine Gaussian SVM model will be used in

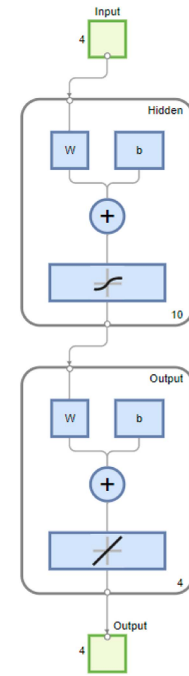


FIGURE 4. Neural network architectural diagram.

the following. Since four outputs are required, the model will be trained four times using the same set of inputs, each time producing a separate model for each output.

- 2) Multiple-input, Multiple-output Regressor Neural Network: This method is designed to produce all outputs simultaneously, generating a single model that can handle multiple outputs. A neural network architecture is designed to accommodate multiple inputs and outputs, as seen in Fig. 4. This architecture contains two hidden layers with varying number of neurons each. It utilizes the Levenberg-Marquardt algorithm, an optimization technique used to solve non-linear least squares problems [34]. This algorithm combines the dual advantages of the gradient descent and the Gauss-Newton methods [34]. Moreover, the adopted neural network also utilizes the hyperbolic tangent (tanh) activation function for the first hidden layer, as represented by (2). Accordingly, a linear activation function, as seen in (3), is used in the second hidden layer of the neural network architecture.

$$f(x) = \tanh(x) = \frac{e^x - e^{-x}}{e^x + e^{-x}} \quad (2)$$

$$f(x) = x \quad (3)$$

In both cases, x is considered to be the input to the activation function, representing the weighted sum of inputs along with a bias.

- 3) Multiple-input, Single-output Regressor Neural Network: This approach follows a similar model as seen in Fig. 4. However, the output layer is designated to

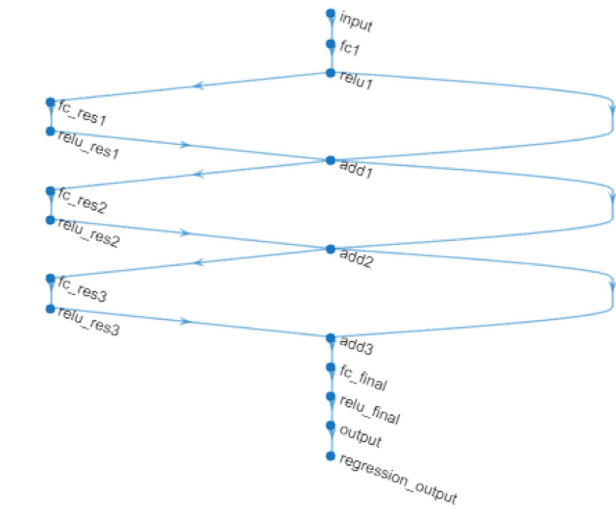


FIGURE 5. ResNet architectural diagram.

- produce only a single output. Hence, similar to the traditional regression approach, this method will also be trained four times, resulting in four distinct models for the outputs. To optimize the parameters and provide accurate results, the number of neurons in each hidden layer will also be varied, and the results are compared accordingly.
- 4) Multiple-input, Multiple-output Residual Neural Network (ResNet): In this approach, the output layer is designed to produce multiple outputs simultaneously, leveraging the capability of ResNets to handle MIMO data efficiently. The architecture is provided in Fig. 5. The skip connections in ResNet help in learning complex relationships between the multiple inputs and outputs by allowing the network to focus on residual mappings [35]. This not only makes training deeper networks more feasible but also improves generalization by reducing the risk of over-fitting [35]. To optimize the parameters and provide accurate results, the number of neurons in each hidden layer is varied, and the performance of different configurations is compared. This approach benefits from the ResNet’s ability to converge faster and maintain high accuracy across all outputs due to its modular and scalable nature.

V. RESULTS

Following the proposed methodology described in the previous section, the traditional regression technique experiments involving the Fine Gaussian SVM are carried out using the MATLAB Classification Learner App. Accordingly, the custom neural network model proposed in Fig. 4, as well as the ResNet in Fig. 5 were also built and trained via MATLAB. Each neural network training phase was completed in 63 epochs, with 6 validation checks. In all experiments, the train and test data were selected at random, and were split 80% - 20%, in favor of the train set.

TABLE 4. Average Differences Per Model and Output

Output	DL(25)	DL(50)	DL(100)	DL(75)	DL(75+50)	ML	Avg. per output
L_{gnd}	2.501	2.672	3.161	2.504	1.497	2.022	2.393
s	31.578	22.271	27.242	59.075	19.097	5.646	27.485
L_v	36.217	14.913	24.095	43.578	17.815	11.687	24.718
L_h	29.854	26.452	45.629	86.850	71.204	47.735	51.287
W_{sub}	2.668	2.333	1.980	4.480	2.547	1.964	2.662
Avg. per model	20.564	13.728	20.421	39.297	22.432	13.811	

A. INITIAL EXPERIMENT: FINE GAUSSIAN SVM VERSUS REGRESSOR NEURAL NETWORK

The first experiment builds on our previous work [16], where we compared various ML techniques in a cascaded format. From these comparisons, we identified the Fine Gaussian SVM as the best-performing model. Moreover, since the outputs in our problem do not need to be fed back as inputs to determine other unknowns, we trained the same model multiple times using the same inputs. Each training session focused on predicting a different output. In this case, the L_{gnd} , s , L_v , L_h , and W_{sub} are considered outputs, while S_{11min} , fc , BW , and $VSWR$, for both bands, are considered as inputs.

The Fine Gaussian SVM results were compared with those of the regressor network, where we employed a traditional training approach with two hidden layers. We varied the number of neurons in these layers to test different configurations:

- 1) 25 neurons per hidden layer
- 2) 50 neurons per hidden layer
- 3) 100 neurons per hidden layer
- 4) 75 neurons per hidden layer
- 5) 75 neurons on the first layer, and 50 neurons on the second layer

Among all configurations, the model is bound to produce a single output per training, hence, as per the Fine Gaussian SVM approach, one regressor model is also trained for each output. Table 4 displays a summarized version of the average difference in percentage form of the actual and predicted values, while Table 5 presents a comparison of predicted and actual values using various models. It displays the actual results obtained in these experiments for the first 10 samples of the test data in a detailed format. The actual column represents the original value, and the predicted values are presented under the specific model types tested. Accordingly, the percentage differences are also provided with each model.

- From these results, we can make two key observations:
- 1) The best performance was achieved with the 50-neuron DL regressor and the Fine Gaussian SVM, both showing an average difference of approximately 14% from the actual values.
 - 2) The outputs for L_{gnd} and W_{sub} had significantly lower error rates compared to the other outputs.

TABLE 5. Comparison of Predicted and Actual Values Using Various Models

Sample	Outputs	Actual	DL (25)	% Diff.	DL (50)	% Diff.	DL (100)	% Diff.	DL (75)	% Diff.	(75+50)	% Diff.	Fine Gauss SVM	% Diff.
1	L_{gnd}	23	21.76	5.38	22.27	3.19	22.27	3.17	22.59	1.77	21.77	5.34	22.31	2.98
	s	1	1.02	2.38	0.69	31.19	0.74	25.99	0.30	69.76	0.25	74.70	0.89	10.92
	L_v	5	6.99	39.78	5.27	5.49	6.26	25.14	4.91	1.86	4.14	17.14	5.23	4.68
	L_h	2	2.31	15.71	3.45	72.28	3.89	94.46	4.26	112.91	6.49	224.72	3.84	92.24
	W_{sub}	46	43.41	5.62	44.51	3.25	44.29	3.71	45.09	1.98	42.83	6.90	44.31	3.67
2	L_{gnd}	21.5	21.62	0.57	22.11	2.84	21.47	0.14	21.94	2.04	21.19	1.45	21.55	0.22
	s	1	1.22	22.34	0.71	28.97	1.51	50.75	0.05	94.93	1.14	13.58	1.07	7.41
	L_v	5	3.19	36.24	6.06	21.12	5.17	3.37	1.63	67.45	4.75	5.10	4.77	4.64
	L_h	4	4.31	7.75	2.09	47.82	4.71	17.65	5.92	48.02	5.88	46.97	4.37	9.35
	W_{sub}	43	43.26	0.61	44.19	2.76	43.11	0.25	44.57	3.66	42.39	1.41	42.70	0.70
3	L_{gnd}	22.5	22.78	1.25	22.75	1.10	22.29	0.91	23.50	4.42	22.67	0.73	21.63	3.87
	s	1	0.51	48.94	0.62	38.42	0.91	9.31	-0.33	133.14	1.06	6.17	1.03	3.41
	L_v	5	4.92	1.55	7.12	42.39	6.14	22.75	2.60	47.92	6.07	21.35	5.44	8.82
	L_h	4	3.54	11.61	1.82	54.56	4.07	1.67	3.41	14.74	2.26	43.39	2.73	31.76
	W_{sub}	45	45.62	1.38	45.74	1.64	45.19	0.42	47.30	5.12	45.70	1.55	43.76	2.76
4	L_{gnd}	23	22.43	2.46	23.19	0.82	22.11	3.85	23.69	2.98	22.90	0.43	21.75	5.43
	s	1	0.54	46.44	0.28	71.80	0.54	46.00	0.24	75.76	1.39	38.96	1.03	2.58
	L_v	5	4.87	2.62	5.10	2.03	8.25	64.93	5.35	6.97	6.28	25.66	5.40	8.00
	L_h	4	2.18	45.56	4.54	13.56	3.43	14.31	3.75	6.38	1.64	58.93	3.36	15.96
	W_{sub}	46	44.91	2.37	46.72	1.57	45.40	1.30	47.44	3.13	47.15	2.49	43.82	4.75
5	L_{gnd}	21.5	22.63	5.27	22.00	2.33	21.77	1.25	21.53	0.12	21.80	1.41	21.91	1.90
	s	1	0.73	26.66	1.03	2.49	0.97	2.59	1.05	4.68	0.94	6.39	1.00	0.21
	L_v	5	6.76	35.12	5.54	10.70	6.25	24.95	8.94	78.74	5.87	17.38	5.85	16.91
	L_h	5	3.71	25.77	3.90	22.08	3.14	37.21	1.64	67.20	3.65	27.05	3.23	35.38
	W_{sub}	43	45.32	5.41	43.88	2.05	43.02	0.04	42.48	1.20	41.72	2.97	43.47	1.24

Further analysis of the dataset reveals that the lower error rate observed is due to the strong correlation between the input values and the changes in L_{gnd} and W_{sub} . In contrast, the other three unknowns have a more complex relationship with the inputs, requiring more sophisticated methods to achieve better accuracy.

B. EXPERIMENT 2: MULTI-OUTPUT REGRESSOR NEURAL NETWORK

To enhance the results, we conducted another experiment using a multi-output regressor neural network model. This model retains the same architecture as shown in Fig. 4, with the key difference being an output layer designed to produce multiple results simultaneously. By doing so, the model also learns the inter-dependencies between the outputs during training, rather than treating each output separately. This approach not only promises potential improvements in accuracy, but also reduces training time, as only one model is needed to generate all outputs. Additionally, the resource requirements for maintaining a single model are significantly lower when compared to multiple models. Finally, getting the results from a multi-output model will require only a single step, as opposed to calling multiple models to get all desired output.

To enhance the experiment, we have also combined the outputs for the two antenna bands including: L_{gnd} , s , d_{offset} , L_v , L_h , W_{sub} , W_v , W_h , L_{TR} , L_{sub} . The results corresponding to 50 samples are provided in Fig. 6(a) to (j), comparing the actual values of the outputs (light blue lines) with the predicted ones (dark blue lines).

Furthermore, Table 6 provides a summarized comparison of the error percentages between the actual and predicted values for each output across the three models.

Upon examining the results, it is clear that the parameter L_{sub} consistently shows an average error rate of 0 across 50 samples. This is because it remains constant throughout the experiments, making it straightforward for the model to learn and predict this value accurately.

On the other hand, the parameter W_h exhibits the highest error rate at approximately 20%. This significant error can also be observed in the dramatic fluctuations of the predicted values from the original values of W_h , as illustrated in Fig. 6(i). This variability introduces a challenge for the model, as the changes in this parameter are not as aligned to the changes in the input data, leading to a higher prediction error compared to other parameters.

Despite the noted observations in parameters W_{sub} and W_h , the overall performance of the models is relatively stable. The average error rate across all 10 outputs falls within a range of 6-8%, indicating a generally acceptable level of accuracy in the predictions. This range suggests that while certain parameters may present more challenges than others, the models are performing well across the majority of the outputs on average.

C. EXPERIMENT 3: MULTI-OUTPUT RESNET

The final experiment evaluates the performance of the Residual Network (ResNet) architecture, as illustrated in Fig. 5, using MIMO data. The results show that ResNet models

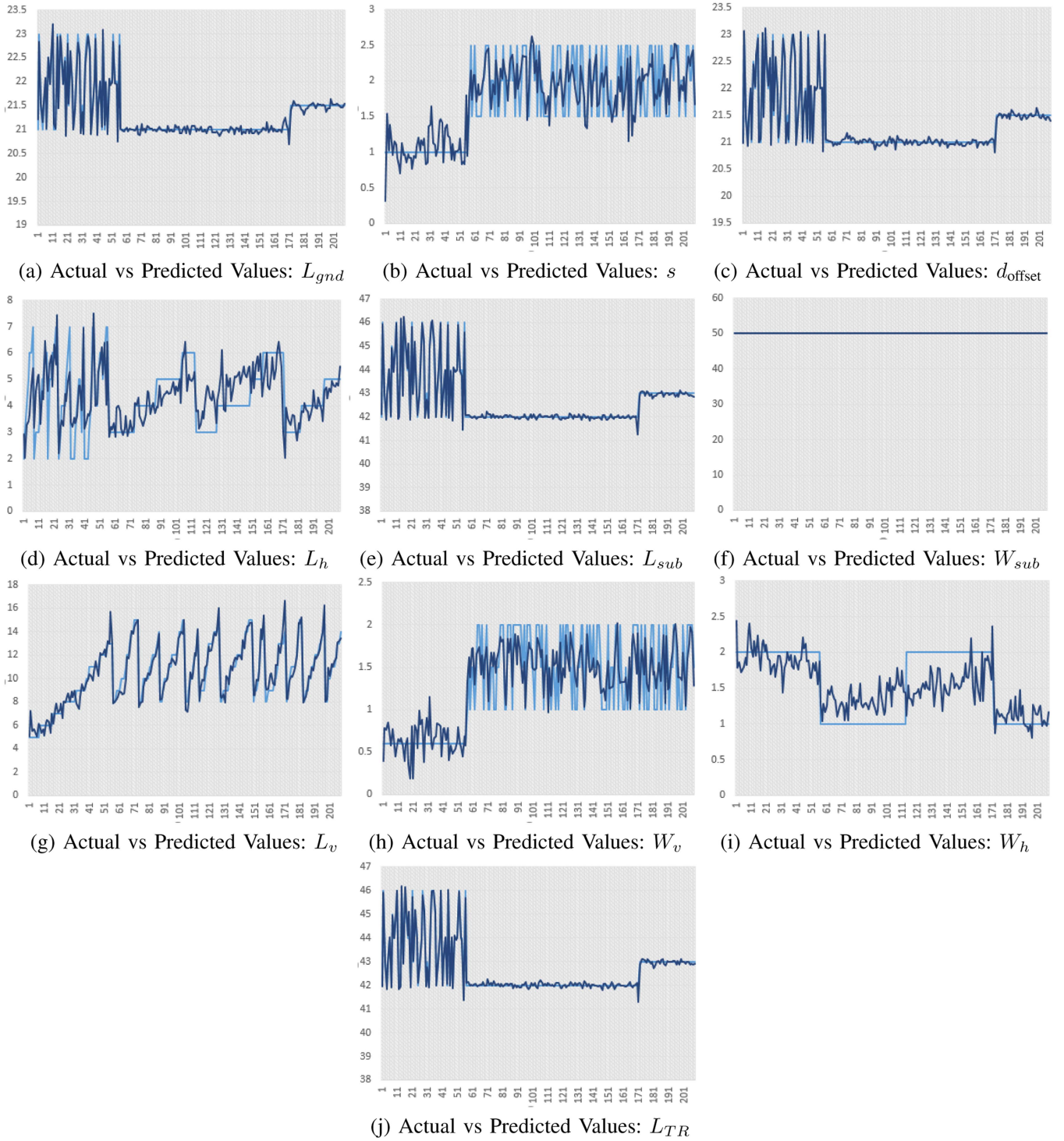


FIGURE 6. Comparison of Actual vs Predicted Values for Different Outputs.

outperform traditional regression learners and the Fine Gaussian SVM in terms of both accuracy and consistency across different outputs. As presented in Table 6, ResNet models configured with 3 and 5 blocks yielded significantly lower error values compared to other models, demonstrating their superior ability to capture the complex relationships within MIMO data. For example, the total error rates for the ResNet

models averaged around 1.27827 and 1.21835, respectively, which are considerably lower than the errors of other models, which ranged from 6.8941 to 7.8501.

Furthermore, ResNet models exhibited better consistency across different outputs, a highly desirable feature for this application. This consistency can be attributed to ResNet's unique architecture, particularly the skip connections, which

TABLE 6. Performance Comparison of Different Models

Category/Model	L_{gnd}	s	d_{offset}	L_h	W_{sub}	L_{sub}	L_v	W_v	W_h	L_{TR}	Total
Regressor Learner (individual)	0.1830	11.7036	0.1601	20.8162	1.3741	0	4.7044	16.3795	20.2139	0.1624	7.5697
Fine Gaussian SVM	0.1071	10.8731	0.1081	15.7317	1.3399	0	4.7134	15.3909	20.5553	0.1212	6.8941
Regressor Learner (group)	0.2831	14.3178	0.2134	17.7336	0.1749	0	5.0957	19.8234	20.6813	0.1784	7.8501
ResNet - 3 blocks (group)	0.2939	0.3112	0.3323	1.7111	1.1663	0	7.1421	0.2711	0.2507	1.304	1.27827
ResNet - 5 blocks (group)	0.3185	0.3161	0.3305	1.5858	1.0992	0	6.8047	0.2818	0.2503	1.1966	1.21835
Average	0.23712	7.10436	0.22888	11.91568	1.03088	0	5.69206	10.42934	12.3903	0.59252	4.9625

enable the network to focus on learning residuals. This, in turn, stabilizes the training process and enhances generalization. Overall, the ResNet models proved more robust and effective in handling the intricate dependencies inherent in MIMO data, leading to more reliable and accurate results than the other approaches tested in this study.

VI. DISCUSSION

The findings from this study demonstrate that ResNet outperform both Fine Gaussian SVM and traditional regressor neural networks for multi-output tasks. ResNet's architecture, with its built-in skip connections, is especially well-suited for managing the complexities of MIMO data. In antenna design, multiple characteristics such as operating frequency, bandwidth, VSWR, gain, directivity, and efficiency are key input data, while several design parameters, including the dimensions of the radiating element, substrate, and parasitic elements like slots or stubs, form the output. For multi-band antennas, the number of output parameters is even higher, given the additional elements required for multi-band functionality. In this context, ResNet represents an ideal choice for AI-based antenna design, not only for L-strip-based dual antennas, as discussed in this article, but also for other types of single or multi-band antennas. By learning residuals, ResNet effectively captures complex relationships between inputs and outputs, leading to more accurate and consistent predictions across all outputs.

One of the major advantages of ResNet for MIMO data is its ability to improve training efficiency and optimize resource use. Unlike traditional approaches that may require separate models for each output, ResNet integrates multiple outputs within a single network. This integration reduces training time, as the model is trained once, and minimizes resource requirements since only one model needs to be maintained. As a result, ResNet not only simplifies deployment but also emerges as a cost-effective solution for complex regression tasks.

Additionally, ResNet addresses the vanishing gradient problem, a common challenge in deep learning models. The residual connections ensure that gradients can flow smoothly through the network during training, enhancing ResNet's ability to capture complex data patterns and improve generalization. ResNet's adaptability and scalability further strengthen

its appeal. The architecture can easily be extended with additional layers to model more complex relationships without significantly increasing computational demands. This scalability is particularly advantageous in dynamic environments, where evolving data distributions require models to remain accurate with minimal adjustments.

While the Fine Gaussian SVM proved effective in scenarios with well-separated data and limited sample sizes, ResNet's flexibility and robustness offer distinct advantages when handling MIMO data, where input-output interactions are more intricate. Although the SVM's use of kernel functions like Gaussian kernels is powerful for capturing non-linear boundaries, it does not provide the depth and versatility that ResNet offers.

All in all, ResNet has emerged as the most effective and efficient methodology for the requirements of this study. Its exceptional performance in managing MIMO data, combined with its benefits in training efficiency, resource management, gradient flow, adaptability, and scalability, solidifies its position as the preferred option for multi-output prediction tasks.

VII. CONCLUSION

This study demonstrates the significant potential of AI, particularly machine learning (ML) and neural networks (NNs), in optimizing the design of dual-band antennas for IoT applications. Although the Fine Gaussian Support Vector Machines (SVM) approach gave favorable results for some of the outputs, the Residual Neural Network (ResNet) emerged as the most effective approach for this application, offering advantages in terms of training efficiency, results consistency, and resource management. This is due to its ability to handle multi-input multi-output (MIMO) data within a single model. This highlights the versatility and effectiveness of each approach, depending on the specific requirements and context of the problem. The integration of AI techniques in antenna design reduces the need for manual tuning, which enables convenient customization for specific frequency ranges or performance characteristics. By treating antenna design as a regression problem, and utilizing important input parameters, the study successfully applied ML and NN models to predict optimal design parameters. This contributes to the enhancement of the design efficiency, as well as time and resource requirements. Ultimately, the selection of the appropriate ML model should be guided by the specific problem requirements

and dataset characteristics. Leveraging the strengths of multiple approaches can also address some modeling challenges. Overall, this research highlights the transformative power of AI in antenna design, opening up more possibilities for more advanced and efficient wireless communication systems in the rapidly growing IoT sector.

Future work should aim to expand the dataset to include a broader range of antenna designs and explore the use of transfer learning to reduce computational costs. Incorporating semi-supervised learning methods and developing hybrid models that combine traditional simulations with AI optimization could further improve model accuracy and efficiency. Additionally, focusing on lightweight architectures would make the models more suitable for real-time applications and resource-constrained environments such as IoT devices.

ETHICAL APPROVAL

Not Applicable

COMPETING INTERESTS

The authors declare no conflict of interest.

AUTHORS' CONTRIBUTIONS

Conceptualization: R. Gadhafi, A. Copiaco; Dataset Generation: R. Gadhafi, H. Mukhtar; Methodology: A. Copiaco; Implementation and Experimentation: R. Gadhafi, A. Copiaco, K. Afsari; Testing: A. Copiaco; K. Afsari; Writing: R. Gadhafi, A. Copiaco, Y. Himeur, K. Ghanem; Proofreading and Review: R. Gadhafi, A. Copiaco, Y. Himeur, H. Mukhtar, K. Ghanem, W. Mansoor; Supervision: R. Gadhafi

FUNDING

This research received no external funding.

AVAILABILITY OF DATA AND MATERIALS

Data will be shared upon request.

REFERENCES

- [1] Y. Sharma, H. H. Zhang, and H. Xin, "Machine learning techniques for optimizing design of double T-shaped monopole antenna," *IEEE Trans. Antennas Propag.*, vol. 68, no. 7, pp. 5658–5663, Jul. 2020.
- [2] A. Alsalemi, Y. Himeur, F. Bensaali, and A. Amira, "Smart sensing and end-users' behavioral change in residential buildings: An edge-based internet of energy perspective," *IEEE sensors J.*, vol. 21, no. 24, pp. 27623–27631, Dec. 2021.
- [3] D. Sharma, B. K. Kanaujia, S. Kumar, K. Rambabu, and L. Matekovits, "Low-loss MIMO antenna wireless communication system for 5G cardiac pacemakers," *Sci. Rep.*, vol. 13, no. 1, 2023, Art. no. 9557.
- [4] N. Sarker, P. Podder, M. R. H. Mondal, S. S. Shafin, and J. Kamruzzaman, "Applications of machine learning and deep learning in antenna design, optimization and selection: A review," *IEEE Access*, vol. 11, pp. 103890–103915, 2023.
- [5] T. Naous, A. Al Merie, S. K. Al Khatib, M. Al-Husseini, R. M. Shubair, and H. M. El Misilmani, "Machine learning-aided design of dielectric-filled slotted waveguide antennas with specified sidelobe levels," *IEEE Access*, vol. 10, pp. 30583–30595, 2022.
- [6] F. Zardi, P. Nayeri, P. Rocca, and R. Haupt, "Artificial intelligence for adaptive and reconfigurable antenna arrays: A review," *IEEE Antennas Propag. Mag.*, vol. 63, no. 3, pp. 28–38, Jun. 2021.
- [7] J. H. Kim and S. W. Choi, "A deep learning-based approach for radiation pattern synthesis of an array antenna," *IEEE Access*, vol. 8, pp. 226059–226063, 2020.
- [8] S. A. Babale et al., "Machine learning-based optimized 3G/LTE/5G planar wideband antenna with Tri-bands filtering notches," *IEEE Access*, vol. 12, pp. 80669–80686, 2024.
- [9] L. Cui, Y. Zhang, R. Zhang, and Q. H. Liu, "A modified efficient KNN method for antenna optimization and design," *IEEE Trans. Antennas Propag.*, vol. 68, no. 10, pp. 6858–6866, Oct. 2020.
- [10] C. Gianfagna, M. Swaminathan, P. M. Raj, R. Tummala, and G. Antonini, "Enabling antenna design with nano-magnetic materials using machine learning," in *2015 IEEE Nanotechnol. Mater. Devices Conf.*, 2015, pp. 1–5.
- [11] N. Kurniawati, F. Arif, and S. Alam, "Predicting rectangular patch microstrip antenna dimension using machine learning," *J. Commun.*, vol. 16, no. 9, pp. 394–399, 2021.
- [12] A. M. Montaser and K. R. Mahmoud, "Deep learning based antenna design and beam-steering capabilities for millimeter-wave applications," *IEEE Access*, vol. 9, pp. 145583–145591, 2021.
- [13] O. Barkat and A. Benghalia, "Optimization of superconducting antenna arrays using RBF neural network," *Int. J. Simul. Multidisciplinary Des. Optim.*, vol. 4, no. 1, pp. 7–10, 2010.
- [14] Q. Wu, W. Chen, Y. Li, H. Wang, J. Yin, and W. Yin, "Machine learning-assisted modeling in antenna array design," in *2024 IEEE Int. Workshop Antenna Technol.*, 2024, pp. 92–93.
- [15] A. I. Hammoodi, M. Milanova, and H. Raad, "Elliptical printed dipole antenna design using ann based on Levenberg-Marquardt algorithm," *Adv. Sci. Technol. Eng. Syst. J.*, vol. 3, no. 5, pp. 394–397, 2018.
- [16] A. Copiaco, R. Gadhafi, H. Mukhtar, and W. Mansoor, "Advancing a cascaded machine learning approach for the accurate estimation of antenna parameters," in *2023 6th Int. Conf. Signal Process. Inf. Secur.*, 2023, pp. 162–166.
- [17] B. Liu, H. Aliakbarian, Z. Ma, G. A. Vandenbosch, G. Gielen, and P. Excell, "An efficient method for antenna design optimization based on evolutionary computation and machine learning techniques," *IEEE Trans. Antennas Propag.*, vol. 62, no. 1, pp. 7–18, Jan. 2014.
- [18] W. Chen, Q. Wu, C. Yu, H. Wang, and W. Hong, "Multibranch machine learning-assisted optimization and its application to antenna design," *IEEE Trans. Antennas Propag.*, vol. 70, no. 7, pp. 4985–4996, Jul. 2022.
- [19] Y. Zhong, P. Renner, W. Dou, G. Ye, J. Zhu, and Q. H. Liu, "A machine learning generative method for automating antenna design and optimization," *IEEE J. Multiscale Multiphys. Comput. Tech.*, vol. 7, pp. 285–295, 2022.
- [20] S. K. Patel, J. Surve, V. Katkar, and J. Parmar, "Machine learning assisted metamaterial-based reconfigurable antenna for low-cost portable electronic devices," *Sci. Rep.*, vol. 12, no. 1, 2022, Art. no. 12354.
- [21] Y. Sharma, X. Chen, J. Wu, Q. Zhou, H. H. Zhang, and H. Xin, "Machine learning methods-based modeling and optimization of 3-D-printed dielectrics around monopole antenna," *IEEE Trans. Antennas Propag.*, vol. 70, no. 7, pp. 4997–5006, Jul. 2022.
- [22] P. Testolina et al., "Enabling simulation-based optimization through machine learning: A case study on antenna design," in *2019 IEEE Glob. Commun. Conf.*, 2019, pp. 1–6.
- [23] Q. Wu, W. Chen, C. Yu, H. Wang, and W. Hong, "Multilayer machine learning-assisted optimization-based robust design and its applications to antennas and array," *IEEE Trans. Antennas Propag.*, vol. 69, no. 9, pp. 6052–6057, Sep. 2021.
- [24] A. Aoad, "Design and manufacture of a multiband rectangular spiral-shaped microstrip antenna using EM-driven and machine learning," *Elektronika ir Elektrotechnika*, vol. 27, no. 1, pp. 29–40, 2021.
- [25] T. Lin and Y. Zhu, "Beamforming design for large-scale antenna arrays using deep learning," *IEEE Wireless Commun. Lett.*, vol. 9, no. 1, pp. 103–107, Jan. 2020.
- [26] Q. Wu, H. Wang, and W. Hong, "Multistage collaborative machine learning and its application to antenna modeling and optimization," *IEEE Trans. Antennas Propag.*, vol. 68, no. 5, pp. 3397–3409, May 2020.
- [27] D. Shi, C. Lian, K. Cui, Y. Chen, and X. Liu, "An intelligent antenna synthesis method based on machine learning," *IEEE Trans. Antennas Propag.*, vol. 70, no. 7, pp. 4965–4976, Jul. 2022.

- [28] X. Chen, J. Wang, and L. Chang, "Extremely low-profile dual-band microstrip patch antenna using electric coupling for 5G mobile terminal applications," *IEEE Trans. Antennas Propag.*, vol. 71, no. 2, pp. 1895–1900, Feb. 2023.
- [29] J. Guo, H. Bai, A. Feng, Y. Liu, Y. Huang, and X. Zhang, "A compact dual-band slot antenna with horizontally polarized omnidirectional radiation," *IEEE Antennas Wireless Propag. Lett.*, vol. 20, no. 7, pp. 1234–1238, Jul. 2021.
- [30] L. H. Ye, Y. J. Li, and D.-L. Wu, "Dual-wideband dual-polarized dipole antenna with T-shaped slots and stable radiation pattern," *IEEE Antennas Wireless Propag. Lett.*, vol. 21, no. 3, pp. 610–614, Mar. 2022.
- [31] Y. Zhang and Y. Zhang, "Dual-band dual-polarized antenna using a simple radiation restoration and decoupling structure," *IEEE Antennas Wireless Propag. Lett.*, vol. 22, no. 4, pp. 709–713, Apr. 2023.
- [32] R. Gadhafi, M. Kannath, H. Mukhtar, and W. Mansoor, "An L-strip double-band and triple-band antenna for WiFi, WiMax and 5G applications," in *2021 IEEE 9th Int. Conf. Inf., Commun. Netw.*, 2021, pp. 107–110.
- [33] J. Li, "Regression and classification in supervised learning," in *Proc. 2nd Int. Conf. Comput. Big Data.*, 2019, pp. 99–104.
- [34] J. J. Moré, "The Levenberg-Marquardt algorithm: Implementation and theory," in *Lecture Notes in Mathematics*, vol. 630. Berlin, Germany, 1978, pp. 105–116.
- [35] K. He, X. Zhang, S. Ren, and J. Sun, "Deep residual learning for image recognition," in *Proc. IEEE Conf. Comput. Vis. Pattern Recognit.*, 2016, pp. 770–778.